

Heredity in one-dimensional quadratic maps

M. Romera, G. Pastor, G. Alvarez, and F. Montoya

Instituto de Física Aplicada, Consejo Superior de Investigaciones Científicas, Serrano 144, 28006 Madrid, Spain

(Received 29 June 1998)

In an iterative process, as is the case of a one-dimensional quadratic map, heredity has never been mentioned. In this paper we show that the pattern of a superstable orbit of a one-dimensional quadratic map can be expressed as the sum of the gene of the chaotic band where the pattern is to be found, and the ancestral path that joins all its ancestors. The ancestral path holds all the needed genetic information to calculate the descendants of the pattern. The ancestral path and successive descendant generations of the pattern constitute the family tree of the pattern, which is important to study and understand the orbit's ordering.

[S1063-651X(98)04212-3]

PACS number(s): 05.45.+b, 87.10.+e

I. INTRODUCTION

According to Crutchfield, Farmer, and Huberman [1], since the first physically motivated study of chaotic dynamics by Lorenz [2], one-dimensional (1D) maps have played a fundamental role in the field's development despite their apparent simplicity. The 1D map obtained from a system of ordinary differential equations captures the essential geometry underlying the chaotic dynamics. Although such a reduction of dimension (from three to one, in Lorenz's case) cannot be uniformly applied to all dynamical systems, for many problems the technique provides more than sufficient heuristic insight into the processes responsible for chaotic behavior [1].

For dissipative dynamical systems that exhibit cascading bifurcations, the dynamics can be described in practice by a 1D map with a single smooth maximum. An example of such maps is provided by 1D quadratic maps as the logistic map $x_{n+1} = \lambda x_n(1 - x_n)$ or the real Mandelbrot map $x_{n+1} = x_n^2 + c$, where λ and c are the corresponding bifurcation parameters. In many experiments, changes in the system behavior are studied as some parameter of the system is varied. Thus much theoretical interest has focused on characterizing the evolution of the dynamics as a function of a system parameter [3]. If we consider a narrow parameter region near the onset of chaos via period doubling (it follows from Feigenbaum's universality [4]), it is natural to expect that an understanding of the behavior of dissipative nonlinear systems in this region may be achieved via detailed analysis of dynamics of 1D maps, in particular, the appearance and coexistence of the periodic orbits.

We have been motivated essentially by a study of the ordering of superstable orbits in the chaotic zone of 1D quadratic maps [5]. As is well known, the periods of the superstable periodic orbits in 1D unimodal maps respond to Sharkovsky's ordering [6,7] $1 < 2 < 4 < \dots < 5 \times 2 < 3 \times 2 < \dots < 5 < 3$, which only orders the periods of the first appearance superstable periodic orbits; therefore, it is a partial ordering.

A complete ordering of the superstable periodic orbits of the 1D unimodal maps, such as the logistic map $x_{n+1} = \lambda x_n(1 - x_n)$, was possible thanks to the work of Metropolis, Stein, and Stein (MSS) [8]. These authors introduced the

concept of a superstable orbit pattern, which allows one to differentiate between orbits with the same period. As is well known, the MSS pattern of a superstable p -periodic orbit $\{x_0, x_1, \dots, x_{p-1}, x_0, \dots\}$, where the initial value x_0 corresponds to the map critical point, is obtained by changing each numerical value x_i ($i > 0$) by the letters L (left) (if $x_i < x_0$) or R (right) (if $x_i > x_0$). In addition, they introduced the concepts of harmonic of a pattern P , $H(P)$, and antiharmonic of a pattern P , $A(P)$, and they enunciated a theorem to calculate the lower period pattern between two given ones, P_1 with parameter λ_1 and P_2 with parameter λ_2 ($\lambda_1 < \lambda_2$), by means of the intersection $H(P_1) \cap A(P_2)$. In such a manner, they ordered periodic orbits as far as period 11 in a pioneer table with 209 patterns [8].

II. ORDERING OF THE ORBITS IN A NONBINARY TREE

Let us consider a 1D quadratic map, like the logistic map $x_{n+1} = \lambda x_n(1 - x_n)$. In Fig. 1(a), we show the graph of the MSS ordering in the neighborhood of the pattern RL^2 , obtained by applying repeatedly the MSS theorem, as done in Ref. [9]. For example, by applying three times this theorem from the patterns RL^2 and RL^3RL (Nos. 94 and 103 of the appendix table of Ref. [8]) the period-10 pattern P_{10} (rounded with a circle in the figure) can be calculated:

$$H(RL^2) \cap A(RL^3RL) = RL^3RL^2,$$

$$H(RL^3RL^2) \cap A(RL^3RL) = RL^3RL^2R,$$

$$P_{10} = H(RL^3RL^2R) \cap A(RL^3RL) = RL^3RL^2RL. \quad (1)$$

We proposed a nonbinary tree as a model of ordering of the superstable periodic orbit patterns in 1D quadratic maps [10], and we gave the rules to compose two patterns of this tree [5]. We proposed this model after carrying out many measurements and verifications on the antenna of the Mandelbrot-like set of the complex form of the 1D quadratic map [10]. In Fig. 1(b), we show the tree ordering of the same pattern RL^2 vicinity as the logistic map in Fig. 1(a), which, as can be seen, does not correspond to a binary tree. This type of nonbinary tree ordering has several advantages in

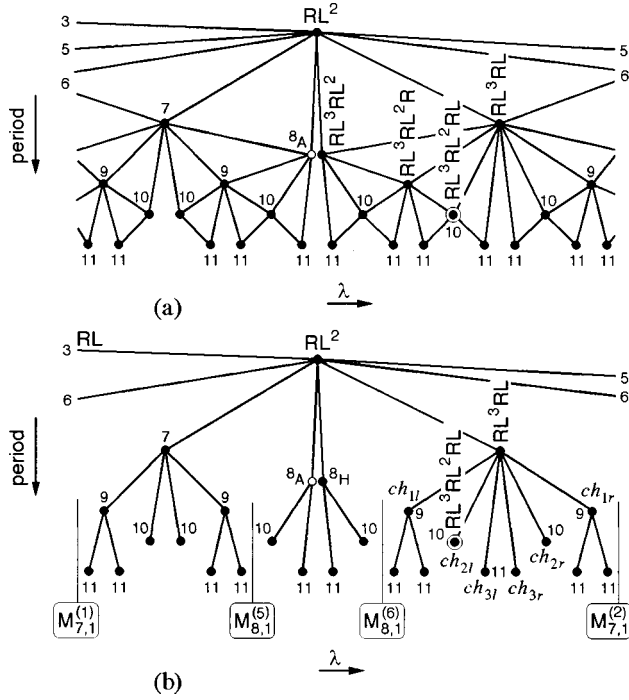


FIG. 1. Pattern generation up to period 11 in the vicinity of the pattern RL^2 of the logistic map $x_{n+1} = \lambda x_n(1 - x_n)$. (a) MSS model. (b) Nonbinary tree model.

relation to the triangular structure graph of MSS: (a) The tree [Fig. 1(b)] is clearer than the graph [Fig. 1(a)]. (b) The tree is structured, and its parts are separated by Misiurewicz points [10]. (c) The development of the three needs an only initial pattern, as we shall see afterwards, whereas the development of the graph needs two initial patterns. (d) It allows one to calculate the patterns in an easy manner. So, pattern P_{10} [Eq. (1)] can be directly obtained from the pattern RL^3RL , by using the method that we show afterwards, with only one easy sum with direction [5]

$$P_{10} = CRL^3RL \overleftarrow{+} CRL = CRL^3RL^2RL,$$

where we add the letter C (corresponding to $x_0 = 1/2$) at the beginning of each MSS pattern so that a pattern of period p has p letters instead of $(p - 1)$ letters [10].

III. HEREDITY CONCEPT

In this work we shall show that the ordering of the orbits in a nonbinary tree allows the introduction of the concept of heredity in the iterative process, whose model is a 1D quadratic map. So, given a pattern P , we can calculate its family tree.

Let us consider a 1D quadratic map. If P is the pattern of a superstable orbit, we say that P is a legal pattern. If P is a pattern that does not correspond to any orbit, we say that P is nonlegal pattern. We can know easily if P is a legal pattern or not by applying the MSS legal inverse path (l.i.p) algorithm [8]: the inverse path of a legal pattern is a l.i.p and the inverse path of a nonlegal pattern is not a l.i.p.

A legal pattern P can be decomposed in an augend P_1 and an addend P_2

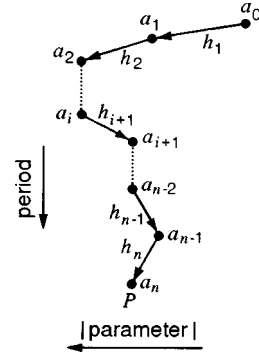


FIG. 2. A sketch of ancestors, heredities, and ancestor path of a pattern P of a 1D quadratic L map.

$$P = P_1 \overrightarrow{+} P_2, \quad (2)$$

where $\overrightarrow{+}$ is the sum with direction $\overleftarrow{+}$ or $\overrightarrow{+}$ [5]. The augend can be either a legal pattern or an F antiharmonic [10] (the only permitted nonlegal pattern in this pattern decomposition). However, the addend must be always a legal pattern. Sometimes, P can be decomposed in several ways; in this case, we can choose any of them without this decision having any influence in the final result.

We say that P_1 is an ‘‘ancestor’’ of P (or P is a ‘‘descendant’’ of P_1), and P_2 , the edge that joins P_1 to P , is the ‘‘heredity’’ that the pattern P_1 transmits to the pattern P , as we shall see afterwards. We use the letter a for ancestors and the letter h for heredities. By successive decompositions as Eq. (2) we have (see a particular case in Fig. 2, which corresponds to an L map [5])

$$P = a_n = a_{n-1} \overleftarrow{+} h_n, \quad a_{n-1} = a_{n-2} \overleftarrow{+} h_{n-1}, \dots, \quad a_1 = a_0 \overleftarrow{+} h_1, \quad (3)$$

where a_{n-1} is the ‘‘father’’ or the closer ancestor of P , and a_0 is the first ancestor or the more remote ancestor of P (a_0 is always a pattern of the period-doubling cascade, which is the gene \mathbf{G} of the chaotic band where P is located [5]). Let us note that expressions (3) are general and therefore the sums have double direction, $\overleftarrow{+}$, while for any particular case, as that shown in Fig. 2, each sum has only one direction. From Eq. (3) we can write the ‘‘ancestral decomposition’’ of P as

$$P = a_0 \overleftarrow{+} \sum h_i, \quad (4)$$

where

$$\sum h_i = h_1 \overleftarrow{+} h_2 \overleftarrow{+} \dots \overleftarrow{+} h_n \quad (5)$$

is the ‘‘ancestral path’’ of pattern P because it is the sum of the edges (heredities) that join the ancestors of P .

Let us note that we have decomposed a given pattern P in the sum of its first ancestor and its ancestral path [Eq. (4)]. The ancestral path holds the genetic information that allows calculating the descendants of P .

We call the first generation of the descendants of a pattern the ‘‘children.’’ For example, in Fig. 1(b) the children of the

pattern RL^3RL are ch_{1r} , ch_{1l} , ch_{2r} , ch_{2l} , ch_{3r} , and ch_{3l} . Usually, the children form couples of the same period, and, in each pair, children are situated on either side of the father. For all the children, both on the right and left, the period is greater the closer to the father. The pattern of a child can be obtained by the sum with direction

$$ch = P \overrightarrow{+} h, \quad ch_r = P \overrightarrow{+} h, \quad ch_l = P \overleftarrow{+} h, \quad (6)$$

where h is the ‘‘heredity’’ that the pattern P transmits to its child ch . By analyzing many experiments where we have studied the descendants of a pattern P , we have deduced that this heredity can be calculated as follows.

Let $a_{i+1} = a_i \overleftarrow{+} h_{i+1}$ be the decomposition of a given ancestor a_{i+1} of P (see Fig. 2). If the sum $\overleftarrow{+}$ has a canonical direction ($\overleftarrow{+}$ for L maps and $\overleftarrow{+}$ for R maps [5]) the decomposition is canonical and the ancestor a_i ($i > 0$) is a ‘‘heredity transmitter’’ to a child of P . If the sum has the anticanonical direction ($\overleftarrow{+}$ for R maps and $\overleftarrow{+}$ for L maps) the decomposition is anticanonical, and the ancestor a_i is not a heredity transmitter to a child of P . However, in this case, the children of the ancestor a_i that have smaller periods than a_{i+1} are heredity transmitters to a child of P .

To calculate all the children of a pattern P , we have to compose P on the right and left with all the heredities h (heredity transmitters), and place the obtained patterns, as we stated above, in such a manner that those with greater periods are closer to the father. It is possible that one or both of the two lower period children of P do not exist. We must verify always that these two patterns are legal patterns. If they are, all the other children are legal patterns; however, if they are not, we must verify if the next lower period children are or are not legal patterns, and so on.

IV. EXAMPLE

Let us apply this model to the period-21 pattern $P = CLRL^4RL^6RL^4RL$ of the real Mandelbrot map located at the parameter value $c = -1.612\,529\,207\,407\,61\dots$. In this case, there are only two possible initial decompositions of the pattern P according to Eqs. (2) or (3). They are

$$P = a_n = CLRL^4RL^6RL^4 \overleftarrow{+} CL \quad (7)$$

and

$$P = a_n = CLRL^4RL^4 \overleftarrow{+} CLRL^4RL. \quad (8)$$

Let us first look at decomposition (7). We have

$$\begin{aligned} a_n &= a_{n-1} \overleftarrow{+} h_n = CLRL^4RL^6RL^4 \overleftarrow{+} CL, \\ a_{n-1} &= a_{n-2} \overleftarrow{+} h_{n-1} = CLRL^4RL^4 \overleftarrow{+} CLRL^4, \\ a_{n-2} &= a_{n-3} \overleftarrow{+} h_{n-2} = CLRL^4RL^2 \overleftarrow{+} CL, \\ a_{n-3} &= a_{n-4} \overleftarrow{+} h_{n-3} = CLRL^2 \overleftarrow{+} CLRL^2, \end{aligned} \quad (9)$$

$$a_{n-4} = a_{n-5} \overleftarrow{+} h_{n-4} = CLR \overleftarrow{+} CL,$$

$$a_{n-5} = a_{n-6} \overleftarrow{+} h_{n-5} = CL \overleftarrow{+} C,$$

$$a_{n-6} = a_{n-7} \overleftarrow{+} h_{n-6} = C \overleftarrow{+} C,$$

$$a_{n-7} = a_0.$$

The ancestor path is

$$\sum h_i = C \overleftarrow{+} C \overleftarrow{+} CL \overleftarrow{+} CLRL^2 \overleftarrow{+} CL \overleftarrow{+} CLRL^4 \overleftarrow{+} CL. \quad (10)$$

It can be useful to rename the ancestors and heredities. As $n=7$ [Eq. (9)], we have $a_{n-6} = a_1, \dots, a_{n-1} = a_6$, and $h_{n-6} = h_1, \dots, h_n = h_7$. It is easy to verify from Eq. (9) that the ancestors a_1 and a_6 are heredity transmitters. Hence, they are composed with P to generate children of P :

$$ch_{1r} = P \overleftarrow{+} a_1 = CLRL^4RL^6RL^4RLRL,$$

$$ch_{1l} = P \overleftarrow{+} a_1 = CLRL^4RL^6RL^4RL^3, \quad (11)$$

$$ch_{4r} = P \overleftarrow{+} a_6 = CLRL^4RL^6RL^4RLRLRL^4RL^6RL^4,$$

$$ch_{4l} = P \overleftarrow{+} a_6 = CLRL^4RL^6RL^4RL^3RL^4RL^6RL^4.$$

It is also easy to verify from Eqs. (9) that the ancestors a_2, a_3, a_4 , and a_5 are not heredity transmitters. In such a case, only their children, with a lower period than the next ancestor, are heredity transmitters. Thus, a_2 has no heredity transmitter, a_3 has only one heredity transmitter $ch(a_3) = CLRL^4$, a_4 has no heredity transmitter, and a_5 has only one heredity transmitter $ch(a_5) = CLRL^4RL^6$. Hence these heredity transmitters have to be composed with P to generate children of P :

$$ch_{2r} = P \overleftarrow{+} CLRL^4 = CLRL^4RL^6RL^4RLRLRL^4,$$

$$ch_{2l} = P \overleftarrow{+} CLRL^4 = CLRL^4RL^6RL^4RL^3RL^4, \quad (12)$$

$$ch_{3r} = P \overleftarrow{+} CLRL^4RL^6 = CLRL^4RL^6RL^4RLRLRL^4RL^6,$$

$$ch_{3l} = P \overleftarrow{+} CLRL^4RL^6 = CLRL^4RL^6RL^4RL^3RL^4RL^6.$$

Figure 3 is a sketch of the family tree of the pattern $P = CLRL^4RL^6RL^4RL$. The ancestors (a_0, \dots, a_6), heredities (h_1, \dots, h_7), and children (of a_3, a_5 , and P) are shown. The periods of ancestors and children are also shown surrounded by a circle.

Let us see now the second decomposition (8). We have (see Fig. 3)

$$P = CLRL^4RL^4 \overleftarrow{+} CLRL^4RL = a_5 \overleftarrow{+} h'_6.$$

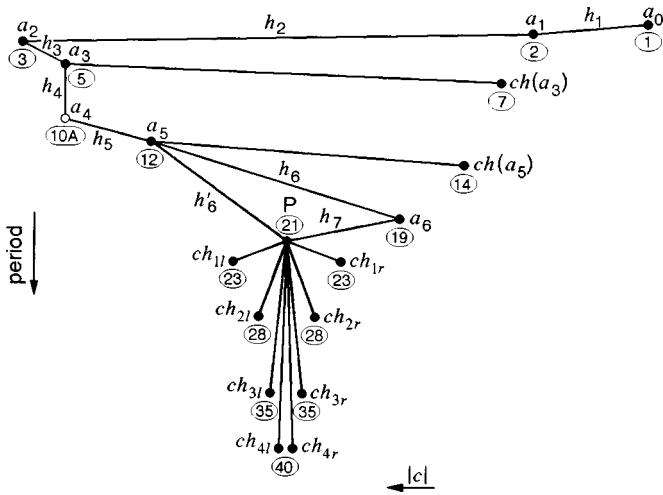


FIG. 3. Ancestors and children of the period-21 pattern $P = \text{CLRL}^4\text{RL}^6\text{RL}^4\text{RL}$ located at the parameter value $c = -1.612\ 529\ 207\ 407\ 61\dots$ of the real Mandelbrot map $x_{n+1} = x_n^2 + c$.

From here on, the decomposition of a_5 is the same as in the former case. It is easy to verify that we obtain the same results through both paths. Indeed, let us note that in the first case [Eq. (7)], a_6 was a heredity transmitter ancestor. Now, in Eq. (8), a_6 is not an ancestor because it is outside the ancestral path; however, it is a heredity transmitter since it is a child of a_5 and it has a period lower than the period of P .

Let us see now a numerical verification of results (11) and (12). By using the Myrberg formula [11] we have calculated the parameters values of all the children of P , from their patterns calculated in Eqs. (11) and (12). The results are shown in Table I. As we can see, all the children are placed close to the father.

The children with a certain period are the closer patterns to the father of all the patterns with that period. As can be numerically checked, the patterns obtained by Eqs. (11) and (12) verify this property; therefore, they are indeed children of P . For example, let us check if the two children of P with the greatest period, ch_{4r} and ch_{4l} (see Fig. 3), are the period-40 patterns closer to P . The total number of period-40 superstable periodic orbits in the chaotic zone of the real Mandelbrot map is huge, 13 743 895 344 orbits according to

TABLE I. Parameter values of the children of the pattern $P = \text{CLRL}^4\text{RL}^6\text{RL}^4\text{RL}$ in the real Mandelbrot map $x_{n+1} = x_n^2 + c$.

Pattern	Period	Parameter value c
ch_{1r}	23	-1.612 437 281 588 79...
ch_{2r}	28	-1.612 504 959 281 62...
ch_{3r}	35	-1.612 523 192 353 40...
ch_{4r}	40	-1.612 527 255 337 07...
P	21	-1.612 529 207 407 61...
ch_{4l}	40	-1.612 531 189 807 37...
ch_{3l}	35	-1.612 535 343 767 13...
ch_{2l}	28	-1.612 555 220 061 27...
ch_{1l}	23	-1.612 652 502 658 42...

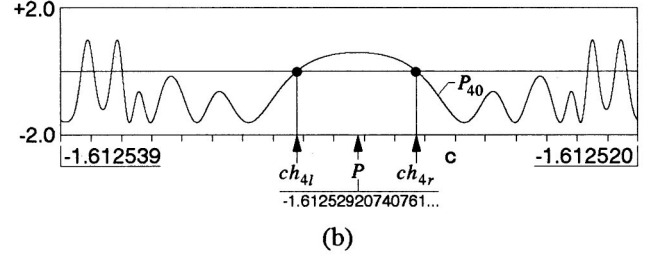
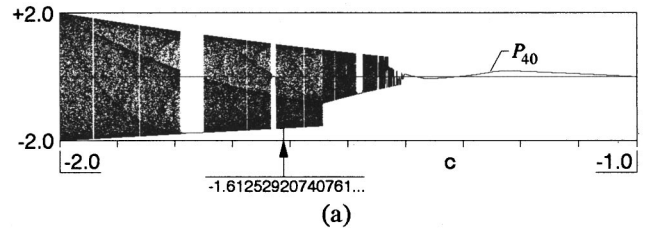


FIG. 4. Critical polynomial P_{40} of the real Mandelbrot map $x_{n+1} = x_n^2 + c$. (a) General view. (b) Detail in the neighborhood of the parameter value $c = -1.612\ 529\ 207\ 407\ 61\dots$

Ref. [12] (most of them near $c = -2$), but two of them are the children ch_{4r} and ch_{4l} , as we shall see next.

As is well known, the parameter values of the superstable periodic orbits of period p are the zeros of the critical polynomial P_p , where $P_0 = 0$, $P_1 = c$, $P_2 = c^2 + c$, $P_3 = (c^2 + c)^2 + c, \dots$. In Fig. 4(a), we depict a general view of the polynomial P_{40} , and in Fig. 4(b) we depict the polynomial P_{40} in the neighborhood of pattern P . We can see that, indeed, ch_{4r} and ch_{4l} are period-40 patterns closer to P . Likewise, we can verify it for the other children of P .

As we can see in Fig. 4(b), in the neighborhood of P the polynomial P_{40} is quasisymmetric with regard to P . Hence each child of any pair of children of a pattern have to be placed symmetrically, one on the right and the other on the left.

Going back to the model, we can repeat the process and calculate the children of each child of P , i.e., the grandchildren or the second generation descendants of P . By repeating this process, we can calculate the third, fourth, etc. generation descendants, obtaining in such a manner a true family tree of the descendants of P .

V. CONCLUSIONS

Given a pattern P , and without any need for other data, we can calculate the complete family tree of such a pattern P . To this end, we first carry out the ancestral decomposition of P [Eq. (4)], and we obtain the ancestors of P . Next, by using the genetic information, which is implicit in the ancestral decomposition, we can generate all the descendants of the pattern P . This study can be extended to all 1D unimodal maps with a negative Schwarzian derivative. The extension of this study to higher dimensional maps will be the goal of future research.

ACKNOWLEDGMENTS

The work was supported by CICYT and DGICYT (Spain) under Research Grant Nos. TIC95-0080, PB94-0045, TEL98-1020, and PB97-1151.

- [1] J. P. Crutchfield, J. D. Farmer, and B. A. Huberman, Phys. Rep. **92**, 45 (1982).
- [2] E. N. Lorenz, J. Atmos. Sci. **20**, 130 (1963).
- [3] C. Grebogi, E. Ott, and J. A. Yorke, Phys. Rev. Lett. RL-TAO**48**, 1507 (1982).
- [4] M. J. Feigenbaum, J. Stat. Phys. **19**, 25 (1978).
- [5] G. Pastor, M. Romera, and F. Montoya, Phys. Rev. E **56**, 1476 (1997).
- [6] A. N. Sharkovsky, Ukr. Mat. Zh. **16**, 61 (1964).
- [7] A. N. Sharkovsky, Yu. L. Maistrenko, and E. Yu. Romanenko, *Difference Equations and their Applications* (Kluwer, Dordrecht, 1993).
- [8] N. Metropolis, M. L. Stein, and P. R. Stein, J. Comb. Theory Ser. A **15**, 25 (1973).
- [9] Y. Ge, E. Rusjan, and P. Zweifel, J. Stat. Phys. **59**, 1265 (1990).
- [10] M. Romera, G. Pastor, and F. Montoya, Physica A **232**, 517 (1996); G. Pastor, M. Romera, and F. Montoya, *ibid.* **232**, 536 (1996); M. Romera, G. Pastor, and F. Montoya, Phys. Lett. A **221**, 158 (1996).
- [11] P. J. Myrberg, Ann. Acad. Sci. Fenn., Ser. AI: Math. **336**, 1 (1963).
- [12] M. Lutzky, Phys. Lett. A **131**, 248 (1988).